5726–5736 *Nucleic Acids Research, 2018, Vol. 46, No. 11* *Published online 10 May 2018*
doi: 10.1093/nar/gky248

Microprocessor depends on hemin to recognize the apical loop of primary microRNA

Tuan Anh Nguyen[1,*,†], Joha Park[2,3,†], Thi Lieu Dang[1], Yeon-Gil Choi[2,3] and V. Narry Kim[2,3,*]

[1]Division of Life Science, Hong Kong University of Science and Technology, Hong Kong, China, [2]School of Biological Sciences, Seoul National University, Seoul 08826, Korea and [3]Center for RNA Research, Institute for Basic Science, Seoul 08826, Korea

Received January 15, 2018; Revised March 23, 2018; Editorial Decision March 26, 2018; Accepted May 03, 2018

ABSTRACT

Microprocessor, which consists of a ribonuclease III DROSHA and its cofactor DGCR8, initiates microRNA (miRNA) maturation by cleaving primary miRNA transcripts (pri-miRNAs). We recently demonstrated that the DGCR8 dimer recognizes the apical elements of pri-miRNAs, including the UGU motif, to accurately locate and orient Microprocessor on pri-miRNAs. However, the mechanism underlying the selective RNA binding remains unknown. In this study, we find that hemin, a ferric ion-containing porphyrin, enhances the specific interaction between the apical UGU motif and the DGCR8 dimer, allowing Microprocessor to achieve high efficiency and fidelity of pri-miRNA processing *in vitro*. Furthermore, by generating a DGCR8 mutant cell line and carrying out rescue experiments, we discover that hemin preferentially stimulates the expression of miRNAs possessing the UGU motif, thereby conferring differential regulation of miRNA maturation. Our findings reveal the molecular action mechanism of hemin in pri-miRNA processing and establish a novel function of hemin in inducing specific RNA-protein interaction.

INTRODUCTION

MicroRNAs (miRNAs) are short, single-stranded RNAs of ∼22 nucleotides (nt), which play a critical role in post-transcriptional gene regulation in various vital biological processes (1–3). Abnormal regulation of miRNA is frequently associated with pathological phenotypes including neurodegenerative diseases and cancer (4–8). Canonical miRNAs are produced through two consecutive processing events by RNase III-type enzymes (3). Nuclear RNase III DROSHA and its cofactor DGCR8 form a complex known as Microprocessor, which cleaves a primary miRNA transcript (pri-miRNA) (Figure 1A) (9–18). The product, a precursor miRNA (pre-miRNA) is a ∼65 nt long hairpin with the characteristic 2 nt overhang at the 3′-end. In the cytoplasm, DICER cleaves pre-miRNA near the apical loop to produce a miRNA duplex of ∼22 nt (19–24). The duplex is loaded onto the Argonaute protein which selects the strand whose 5′-end is uridine or adenosine and thermodynamically unstable (25). DICER acts as a molecular ruler to measure a set distance (22 nt) from the pre-miRNA termini that are generated by Microprocessor in the first processing step. Therefore, Microprocessor predetermines the sequence and function of the final products.

A pri-miRNA has a local stem-loop, consisting of a stem of about three helical turns with an apical loop and single-stranded RNA (ssRNA) segments at the base of the stem (Figure 1A) (3,13). Microprocessor recognizes pri-miRNAs by interacting with multiple cis-elements in the substrate (15,18). DROSHA, the catalytic subunit, recognizes the basal elements: the basal junction (the single-stranded RNA-double-stranded RNA junction at the base) and the basal UG motif. DROSHA locates its catalytic center at ∼11 bp from the basal junction and executes simultaneous cleavages on two strands. Another essential component, DGCR8 joins Microprocessor as a dimer to create a heterotrimeric complex (Figure 1A). DGCR8 stabilizes DROSHA protein through the C-terminal tail (CTT) and enhances RNA binding affinity of Microprocessor through its double-stranded RNA (dsRNA) binding domains (dsRBDs). DGCR8 also places DROSHA at the expected cleavage sites, thereby preventing misorientation or dislocation that results in unproductive (abortive) or alternative cleavage, respectively (15). The DGCR8-RNA interaction is well established as a critical factor for pri-miRNA processing *in vitro* and *in vivo* (15,26–29). However, the mechanism underlying the achievement of specific RNA recognition and discrimination among different pri-miRNAs in this processing step is unknown.

Heme, which consists of a ferrous ion (Fe^{2+}) at the center of a porphyrin ring, is an essential cofactor for various proteins and enzymes. It serves as an important structural com-

*To whom correspondence should be addressed. Tel: +82 28809120; Fax: +82 28870244; Email: narrykim@snu.ac.kr
Correspondence may also be addressed to Tuan Anh Nguyen. Tel: +852 34692679; Fax: +852 23581552; Email: tuananh@ust.hk
†The authors wish it to be known that, in their opinion, the first two authors should be regarded as Joint First Authors.

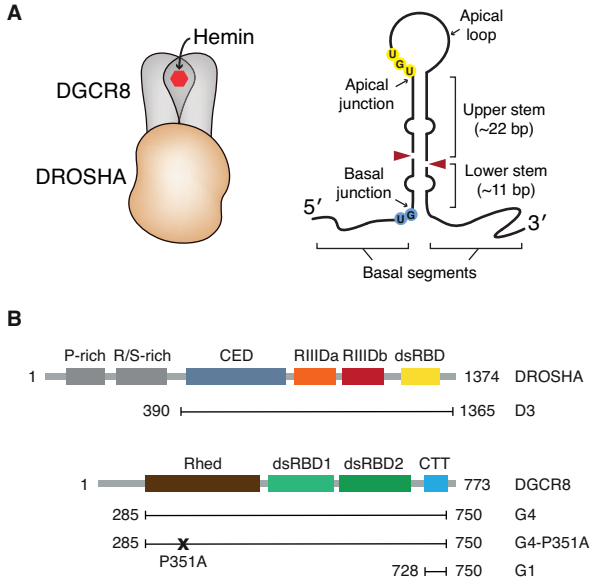

Figure 1. Human Microprocessor complex and pri-miRNA. (**A**) Microprocessor is a trimeric complex that consists of one DROSHA and a DGCR8 dimer. Hemin, a ferric form (Fe^{3+}) of heme, associates with the DGCR8 dimer. A typical pri-miRNA, the substrate of Microprocessor, has a stem-loop structure. The apical UGU motif of pri-miRNA is recognized by the DGCR8 dimer. The brown arrowheads indicate the DROSHA cleavages. (**B**) Protein constructs used in this study. The first and end residue numbers for each construct are shown. The mutation site is marked by 'x'. P-rich: Proline-rich domain, R/S-rich: Arginine/serine-rich domain, CED: central domain, RIIIDa and RIIIDb: RNase III domains, dsRBD: dsRNA-binding domain, Rhed: RNA-binding heme domain, CTT: C-terminal tail region.

ponent for the formation of hemoglobin, myoglobin, and cytochrome complexes. Heme is also a critical cofactor for numerous enzymes such as catalases, cyclooxygenases, and nitric oxide synthases (30–34). Hemin, a ferric form (Fe^{3+}) of heme, is incorporated in a DGCR8 dimer and stimulates the Microprocessor activity *in vitro* (26–28) and *in vivo* (29). The addition of a hemin precursor (5-aminolevulinic acid, ALA) in *Escherichia coli* culture overexpressing DGCR8 could induce the formation of the DGCR8 dimer over the monomeric form (26–28), indicating that hemin enhances dimerization of DGCR8. Furthermore, the hemin level in human cells affects the expression of several miRNAs (29), supporting the physiological function of hemin in stimulating miRNA biogenesis.

Despite the importance of hemin in pri-miRNA processing, its action mechanism remains unclear since it is challenging to recapitulate DGCR8-RNA binding *in vitro* which mimics the original biochemical context; the interaction of DGCR8 with RNA markedly differs when DGCR8 is alone or in a complex with DROSHA (15,26,35). For example, DGCR8 alone interacts with pri-miRNAs with various stoichiometry ranging from two to three DGCR8 dimers per one pri-miRNA, suggesting that DGCR8 may contact two or three different positions of pri-miRNAs and that multiple hemin molecules may participate in a sequence-independent manner (15,26,35). However, our latest results (15) using the purified Microprocessor complex showed that only one DGCR8 dimer interacts with one pri-miRNA (Figure 1A), implying that one hemin molecule might be involved. These findings prompted us to test if hemin might act on a particular element to mediate the specific interaction between DGCR8 and pri-miRNAs. Interestingly, hemin was recently reported to induce a conformational change of DGCR8 and enhance the accuracy of pri-miRNA processing (36).

In this study, we explored the action mechanism of hemin using purified recombinant Microprocessor (15). We discovered an interesting role of hemin in enhancing the specificity of the RNA-binding activity of a DGCR8 dimer. Furthermore, our genome editing and genome-wide sequencing data indicate that hemin could play regulatory roles by differentiating the maturation rates of miRNAs.

MATERIALS AND METHODS

Processing assay

The processing assay was carried out at 37°C in 20 μl assay buffer containing 50 mM Tris-hydrochloride (Tris–HCl, pH 7.5), 150 mM sodium chloride (NaCl), 10% glycerol, 0.2 μg/μl bovine serum albumin (BSA), 1 mM dithiothreitol (DTT), and 2 mM magnesium chloride ($MgCl_2$). Approximately 10 000 cpm of the RNA substrates was used, and the enzyme concentrations and incubation time are indicated in the figures. The reaction was stopped by adding 20 μl TBE-urea sample buffer (Bio-Rad) and immediately chilling the mixture on ice. Finally, the mixture was heated at 95°C for 10 min and quickly chilled on ice before being loaded onto a 10% Urea-polyacrylamide gel electrophoresis (Urea-PAGE) gel with the RNA size markers (Decade marker, Ambion). The RNA substrates were prepared by the *in vitro* transcription using MEGAscript T7 Kit (Ambion). The substrates were either internally labeled with [α-^{32}P] UTP or end-labeled with [γ-^{32}P] UTP.

Recombinant protein purification

The D3–G1 complex was purified as described previously (15,18). To purify the DGCR8 proteins, we used T500 buffer containing 20 mM Tris–HCl (pH 7.5), 500 mM NaCl and 2 mM β-mercaptoethanol, supplemented with 2 μg/ml RNase A, 2 μg/ml staphylococcal nuclease, 5 mM calcium chloride ($CaCl_2$) and a protease inhibitor cocktail. The gene fragment encoding G4-P351A fused to an N-terminal 10× His-sfGFP tag was cloned into the pET-28a vector and overexpressed in BL21(DE3)-CodonPlus-RIPL by IPTG induction at 16°C. The cell lysate was prepared in T500 buffer and loaded on a Ni-NTA column equilibrated with the same buffer. The column was washed in tandem with T2000 (20 mM Tris–HCl [pH 7.5], 2000 mM NaCl, 2 mM β-mercaptoethanol) containing 40 mM imidazole and T300 (20 mM Tris–HCl [pH 7.5], 300 mM NaCl, and 2 mM β-mercaptoethanol) containing 40 mM imidazole. The proteins were eluted with T300 containing 200 mM imidazole, and the buffer was immediately changed to T300 using a desalting column. The protein sample was treated with 10× His-tagged HRV 3C protease at 4°C overnight and loaded on a second Ni-NTA column to remove the sfGFP tags and the protease. The unbound fraction and the wash fraction with T300 containing 20 mM imidazole

were collected and concentrated using a 30-kDa molecular weight cutoff (MWCO) centricon. Then, 2.5 mg of G4-P351A was fractionated using a Superdex 200 10/300 GL column (GE Healthcare). Two major peaks corresponding to monomeric and dimeric G4-P351A were collected separately. Another 2.5 mg of G4-P351A was supplemented with 20 μmol of hemin (Sigma-Aldrich), and the mixture was incubated on ice for 1 h prior to loading on the Superdex 200 10/300 GL column. The major peak corresponding to dimeric G4-P351A was collected. The presence of hemin in the G4-P351A dimer was confirmed by its spectra. The purified proteins were liquid nitrogen (LN2)-cooled and stored at −80°C.

Purification of recombinant DGCR8 from human cells

The DG4 fragment of DGCR8 (amino acid [aa] 285–773) fused to the C-terminal GFP and 10× His-tag was cloned into the pXG plasmid as used in the previous study (15). The cloned plasmids were transfected into 4 l HEK293E suspension cell culture and the cells were harvested after 4 days. The cell pellets were resuspended in 200 ml T500 buffer containing 20 mM Tris–HCl (pH 7.5), 500 mM NaCl, and 4 mM β-mercaptoethanol, supplemented with 2 μg/ml RNase A and a protease inhibitor cocktail. The clear lysate obtained by sonication and centrifugation was loaded on a Ni-NTA column. The column was washed with 200 ml T500 containing 20 mM imidazole and eluted with 50 ml T500 containing 200 mM imidazole. The eluates were treated with 50 μg Rhinovirus (HRV) 3C protease overnight at 4°C to completely separate DG4 from the protein GFP and His tags. The cleaved proteins were diluted to 100 mM NaCl with T0 containing 20 mM Tris–HCl (pH 7.5) and 4 mM β-mercaptoethanol and bound with SP-sepharose. The SP-sepharose was washed with 150 mM NaCl-containing buffer, and the proteins were eluted with T500. The proteins were further purified using gel filtration with a Superdex 200 10/300 GL column. The proteins were finally frozen with LN2 and stored at −80°C.

Reconstitution D3-G4G4-P351A complex with hemin

D3 fused with protein G (D3-proG) was purified in the complex with CFP-fused G1 (G1-CFP) using the Ni-NTA column and Mono-Q sepharose as previously described (15). The 1000 pmol of the purified D3-proG-G1-CFP proteins were bound to IgG-sepharose and were subsequently added with 750 pmol of the G4G4-P351A (the dimer form). The mixture was incubated at 4°C for 1 h to allow the formation of the D3-proG-G4G4-P351A complex and then it was washed with T500 containing 20 mM Tris–HCl (pH 7.5), 500 mM NaCl, and 2 mM β-mercaptoethanol to wash out the unbound G4G4-P351A. The D3-proG-G4G4-P351A-bound beads were divided into two halves and one was supplemented with 1000 pmol hemin. After a 1-h incubation with hemin at 4°C, the unbound hemin was removed by washing the beads with T500 buffer. Finally, 2 μg of HRC-3C was added to release the D3-G4G4-P351A by cleaving the 3C-cleavage site located between D3 and protein G.

Rescue experiments and qPCR

The DGCR8-KO cells were maintained in McCoy's 5A medium supplemented with 10% fetal bovine serum (FBS). Then, 5 μg of the plasmid was transfected into 30% confluent cells in a 60-mm dish using 6 μl Lipofectamine 3000 (Invitrogen). After 2 days, the total RNA was isolated from the transfected cells using TRIzol, and 50 ng was used in the qPCR experiments using the Taqman kit for miRNAs. The cDNAs for the qPCR of pri-mir-16-1 were synthesized from 1 μg of total RNA using random hexamer primers as reverse transcription primers and SuperScript III (Life Technologies). The specific PCR primers for pri-mir-16-1 were used in real-time qPCR using SYBR qPCR premix (Applied Biosystems).

Western blot and immunoprecipitation

The cells were lysed in 150 mM NaCl, 20 mM Tris–HCl at pH 7.5, 1 mM DTT, and protease inhibitor cocktails by sonication. The cell lysates were collected by centrifugation at full speed. The laboratory-made mouse DROSHA antibody was used to capture DROSHA. The immunoprecipitated materials and cell lysates were analyzed using Western blot with a Cell Signaling antibody (#3364) for DROSHA and laboratory-made mouse antibody for DGCR8.

Small RNA sequencing analysis

Small RNA sequencing libraries for the HCT116 and DGCR8 knockout cells were prepared as described previously (37). Sequencing reads were preprocessed using cutadapt (38); 3′ adapter sequences were trimmed, and low quality reads (<18 nt, <20 Phred score for 5% of the read) were discarded. High quality reads were collapsed and mapped to the human genome (hg38) by Bowtie2 aligner that allows multimapping (39). The reads that mapped to the miRNA loci were collected. These mapped reads that had no mismatches in the region from the 5′-end to 3 nt inward from the 3′-end were counted for further analysis. The read counts of miRNAs were normalized to reads per a million (rpm) and were re-scaled to obtain relative abundance to the geometric mean of the non-canonical miRNAs (hsa-mir-320a, hsa-mir-320b-1, hsa-mir-320c-1) that bypass Microprocessor processing. In the rescue experiments, normalized expression values of the biological replicates were aggregated by taking the mean. The deep sequencing data from this study were submitted to the Gene Expression Omnibus (GEO: http://www.ncbi.nlm.nih.gov/geo/) under the accession number GSE111431.

RESULTS

Hemin precisely positions Microprocessor on pri-miRNA

To examine the potential effects of hemin on pri-miRNA processing, we used the DGCR8-P351A mutant (proline at 351 to alanine) that can be expressed as a stable apoprotein dimer without hemin in *E. coli* (Figure 1B) (27). This mutant protein can be subsequently reconstituted with synthetic hemin *in vitro*, which enables the comparison of the activity of DGCR8 dimer in the presence or absence of

hemin. The G4-P351A fragment (covering all the essential domains of DGCR8) was first purified as described in 'Materials and Methods', and fractionated further by using gel filtration column to examine the dimeric status and hemin binding capacity. The G4-P351A proteins were separated into monomer and dimer peaks as monitored by absorbance at 280 nm (black line, Figure 2A), and neither of these two peaks showed the hemin signal as determined by absorbance at 450 nm (black line, Figure 2B), suggesting that the proteins purified from *E. coli* did not associate with hemin. However, when the same proteins were incubated with synthetic hemin, they were separated into monomer and dimer peaks by gel filtration (red line, Figure 2A), out of which only the dimer peak showed the hemin signal (red line, Figure 2B). This result indicates that the G4-P351A dimer can be successfully incorporated with hemin *in vitro*. The ratio of dimer over monomer increased in the hemin-supplemented G4-P351A sample, suggesting that hemin might stabilize or stimulate the dimer formation (26–28). In order to obtain a large amount of protein for pri-miRNA processing assays, 2.5 mg of the purified G4-P351A protein with or without hemin supplement was fractionated by a larger gel filtration column, a Superdex 200 10/300 GL column (Supplementary Figure S1). The G4-P351A dimer proteins without hemin (G4G4-P351A, fraction 25 of Supplementary Figure S1A) and with hemin (G4G4-P351A-hemin, fraction 25 of Supplementary Figure S1B) were collected and used for processing assays throughout this study.

The activity of G4G4-P351A was measured by incubation with DROSHA and internally labeled pri-mir-30a in processing assay. Note that DROSHA (the D3 fragment covering all essential parts of DROSHA) was co-expressed with the DGCR8 G1 fragment (the C-terminal tail) which stabilizes DROSHA and can be replaced effectively by G4 (15). G4G4-P351A could assist DROSHA in cleaving the substrate more efficiently than the monomer, but the processing was imprecise, yielding a number of alternative and unproductive cleavage products (Figure 2C, lanes 6–7). In contrast, hemin-containing G4G4-P351A dramatically enhanced the productive cleavage of DROSHA, while blocking the unproductive and alternative cleavage events (Figure 2C, lanes 9–10). These results indicate that the specific RNA-binding activity of the DGCR8 dimer is kept idle until hemin is incorporated.

To affirm the role of hemin in pri-miRNA processing and exclude the possibility of its affecting the reconstitution efficiency of Microprocessor, we reconstituted Microprocessor using a different method (Figure 2D). In brief, the D3-G4G4-P351A complex was first reconstituted by mixing D3-G1 on the IgG-sepharose beads with G4G4-P351A. Subsequently, the resulting complex was supplemented with hemin. The free hemin was then washed away, and the hemin-incorporated complex was eluted from the beads using HRV-3C proteases for the subsequent assay with end-labeled pri-mir-30a (Figure 2D). The 'specificity' of processing was calculated as the ratio of the productive products (F1) over the sum of the alternative (F1″) and unproductive (F1′) products. The results showed that hemin enhances the specificity of Microprocessor by promoting processing at the correct orientation and position.

Hemin assists the UGU recognition by DGCR8

We previously proposed that the DGCR8 dimer recognizes the UGU motif located at the apical loop (15). To determine if hemin is involved in the UGU recognition, we carried out *in vitro* processing assay using a pri-miRNA mutant lacking the UGU motif (Figure 3A, Pri-mir-30aΔUGU). While the processing of wild-type substrate was increased dramatically by hemin, that of the ΔUGU mutant was only modestly enhanced by hemin (Figure 3B and C). Of note, the additional substitution of C with U in the apical loop of the ΔUGU mutant is to maintain an intact structure of the loop, since pri-mir-30a may take alternative conformations (Supplementary Figure S2A). Another UGU mutant (Pri-mir-30aΔUGU-2) that maintains C at the apical loop also showed a similarly compromised specificity (Supplementary Figure S2B–D). These results suggest that hemin can facilitate the specific interaction between DGCR8 and the UGU motif.

Moreover, a comparable result was observed with an artificial pri-miRNA (Figure 3D–F) that was reconstructed from the sequences that share no homology to any known pri-miRNAs (13,15). Hemin increased the cleavage specificity more drastically in the presence of the UGU motif than in its absence. This result indicates that hemin depends, at least partially, on the UGU motif in specifying the RNA-DGCR8 interaction.

DGCR8 associates with hemin in human cells

Although hemin was found to associate with DGCR8 when proteins were expressed in *E. coli*, it has not yet been demonstrated that hemin is also incorporated into DGCR8 in human cells. To clarify this issue, we optimized the conditions for expression and purification of a high amount of DGCR8 proteins from human cells. The purified DGCR8 proteins displayed a brown color (Supplementary Figure S3A) similar to the proteins purified from *E. coli* (26), suggesting that the DGCR8 proteins in human cells also interact with hemin. In addition, the proteins fractionation using the gel filtration column showed that the peak of protein signal (A280) was coincident with that of the hemin signal (A450) (Supplementary Figure S3B and C). This indicates that DGCR8 indeed interacts with hemin in human cells.

Generation of DGCR8 knockout cell line

To examine the cellular effect of hemin, we ectopically expressed DGCR8 (WT or mutant) and compared their effects on miRNA biogenesis. To avoid any interference from endogenous DGCR8 proteins, we created the DGCR8 knockout (KO) cells using the HCT116 cell line. We initially tried to knockout DGCR8 by targeting the genomic DNA sequence encoding its N-terminal region containing the start codon; however, this approach did not produce any knockout colonies. We then targeted the DNA region encoding the C-terminal region of DGCR8 containing DROSHA-interacting domain, CTT. Sequencing of the genomic DNA extracted from the isolated single-cell clone verified the deletion mutations at the targeted regions (Figure 4A, ΔCTT). Western blot analysis using two different antibodies against DGCR8 detected the expression of

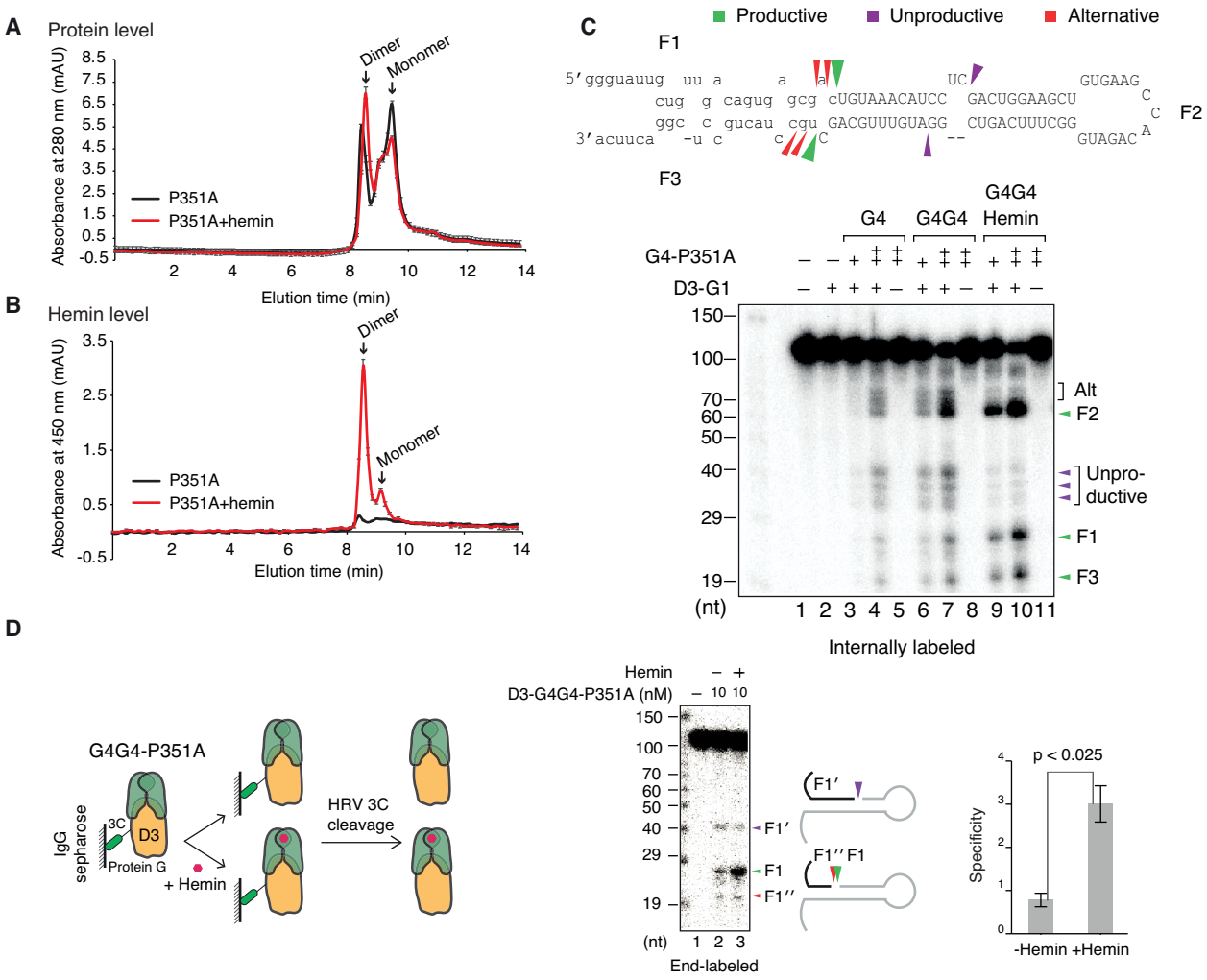

Figure 2. Hemin enhances efficiency and accuracy of pri-miRNA processing. (**A**, **B**) The high performance liquid chromatography (HPLC) profiles of the purified DGCR8 proteins. The purified G4-P351A proteins without or with hemin addition were loaded on an Agilent AdvanceBio SEC300Å column run with the Agilent 1260 Infinity II Quat LC system. The protein (A) and hemin levels (B) were monitored by the absorbance at A280 nm and A450 nm, respectively. The experiments were repeated three times. (**C**) The increased specificity of DROSHA by hemin-associated G4G4-P351A. Microprocessor can process pri-mir-30a at the productive (indicated with the green arrowheads), unproductive (indicated with the purple arrowheads) or alternative sites (indicated with the red arrowheads). G4G4-P351A was incubated with the excessive amount of hemin and resulting G4G4-P351A-hemin was subsequently separated from free hemin by the gel filtration column. The G4G4-P351A proteins without and with hemin were mixed with the D3-G1 complex to obtain D3-G4G4-P351A and D3-G4G4-P351A-hemin, respectively. The pri-mir-30a was internally labeled and processed at 150 mM NaCl for 60 min by 0.25 μM of D3-G1 and increasing amounts of G4G4-P351A (0.03 and 0.06 μM). F1, F2 and F3 are the productive products. 'Alt' is abbreviation of alternative. The protein names are indicated in the figure. (**D**) The increased specificity of Microprocessor reconstructed with hemin. The D3-G4G4-P351A was first reconstituted on the IgG sepharose through the protein G tag of D3. Hemin was then added to the reconstituted complex. The excessive amount of hemin was removed and the hemin-incorporated complex was released from beads by the HRV 3C cleavage between protein G and D3. The pri-mir-30a processing assay was carried similarly as described in (C), except that pri-mir-30a was 5′-end labeled.

the DGCR8 fragment of reduced size (Figure 4B and Supplementary Figure S4A), demonstrating the loss of the C-terminal region. To confirm whether the shortened DGCR8 fragment fails to interact with DROSHA, we performed co-immunoprecipitation and gel filtration fractionation (Figure 4B and Supplementary Figure S4B). The data clearly demonstrated that the DGCR8 fragment in the edited cells (ΔCTT) does not associate with DROSHA. Furthermore, the *DGCR8* mRNA level was increased in the ΔCTT cells (Supplementary Figure S4C). The *DGCR8* mRNA is normally cleaved by Microprocessor, which is required for the homeostatic maintenance of Microprocessor activity (40). But this feedback control fails in the ΔCTT cells because the DGCR8ΔCTT protein cannot form functional Microprocessor. Finally, the level of mature miR-16-1 (Figure 4C) or miR-30a (Supplementary Figure S4D) was markedly reduced in the ΔCTT cells while the pri-mir-16-1 level increased in the ΔCTT cells (Figure 4C). Consistently, the abundance of canonical miRNAs relative to that of non-canonical miRNAs (such as miR-320a) was strongly reduced in the ΔCTT cells as measured by small RNA sequencing (Figure 4D), indicating the functional ablation of Microprocessor.

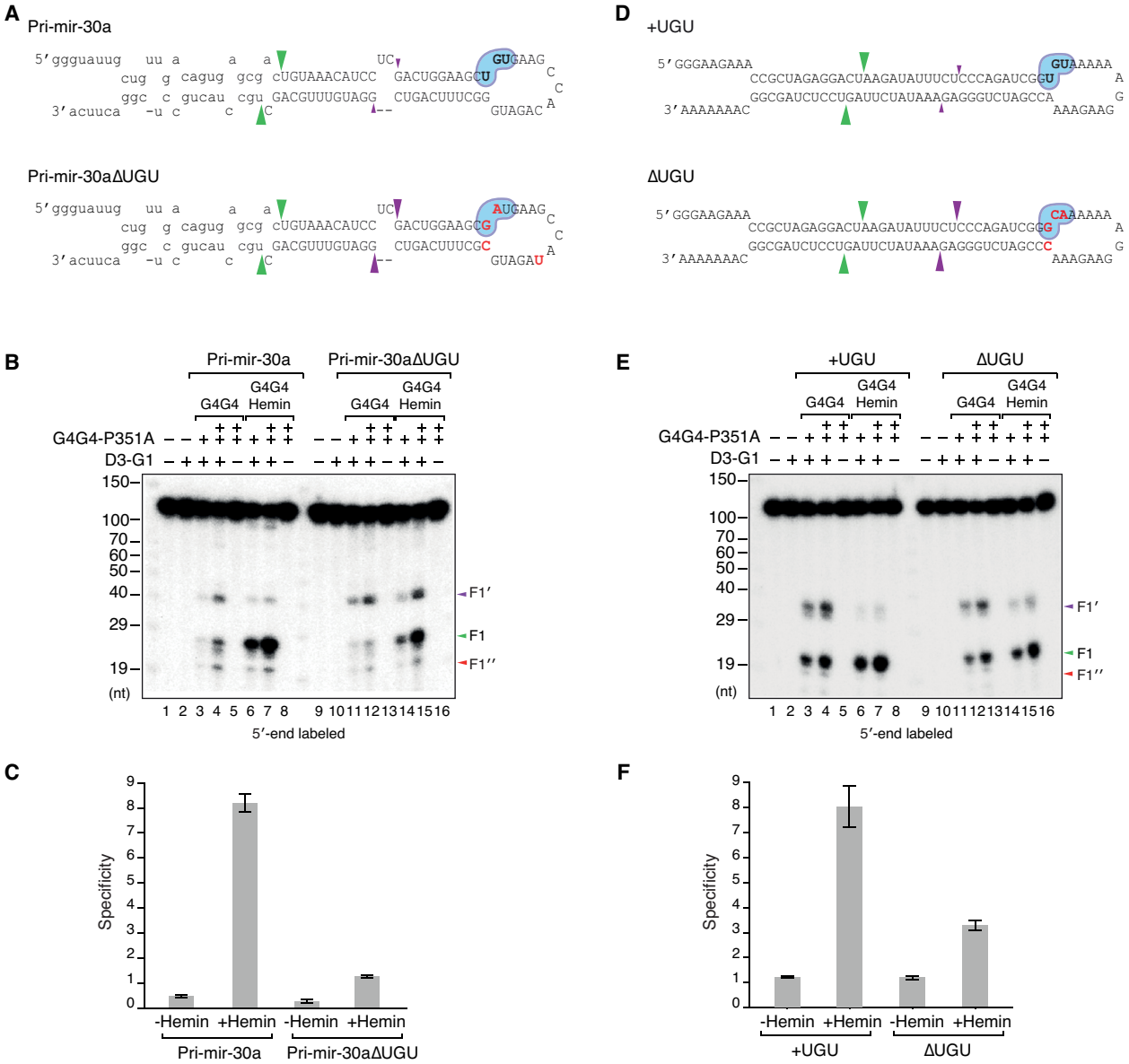

Figure 3. Hemin activates the UGU recognition of DGCR8. (**A**) The pri-mir-30a substrates. The mutated nucleotides are in red. The size of the arrowhead roughly indicates the relative processing efficiency of D3-G4G4-P351A with hemin for each substrate. The green and purple arrowheads indicate the productive and unproductive cleavages, respectively. (**B**) Processing of pri-mir-30a by Microprocessor. Pri-mir-30a (WT) and pri-mir-30aΔUGU were processed at 150 mM NaCl for 60 min by 0.25 μM of D3-G1 and increasing amounts of G4G4-P351A (0.03 and 0.06 μM). The protein names are indicated in the figure. (**C**) The quantification of the data from B. The densities of the bands were measured by the Multi Gauge V3.0 (FUJIFILM). The ratio of the productive products (F1) over the combination of the unproductive (F1′) and alternative (F1″) products was calculated from the three independent experiments and plotted on the bar graph. The average ratio ± standard error of the mean from the three independent experiments are shown. (**D**) The artificial substrates with or without the UGU motif are illustrated as pri-mir-30a in A. (**E**) Processing of the artificial substrates by Microprocessor. The +UGU and ΔUGU were processed at 150 mM NaCl for 60 min by 0.25 μM of D3-G1 and increasing amounts of G4G4-P351A (0.03 and 0.06 μM). The protein names are indicated in the figure. (**F**) The quantification of the data from E as described in C.

Hemin differentiates miRNA maturation

The P351A mutant can dimerize but does not show effective hemin binding (27,28) while the C352A mutant (cysteine at 352 to alanine) is impaired in both dimerization and hemin-binding (26). Using these mutants, we investigated if the UGU motif determines the sensitivity of the pri-miRNA processing towards cellular hemin concentration. We selected pri-mir-16-1 (lacking UGU) and pri-mir-30a (containing UGU) to test this hypothesis. The plasmids containing the DGCR8-WT, DGCR8-C352A, or DGCR8-P351A allele were transfected into the ΔCTT cells, and miRNA levels were measured using quantitative polymerase chain reaction (qPCR, Figure 5A). We found that both the WT and P351A (which can dimerize) enhanced the overall expression of miRNAs more efficiently than the C352A did (Figure 5B). This is consistent with the *in vitro* observation

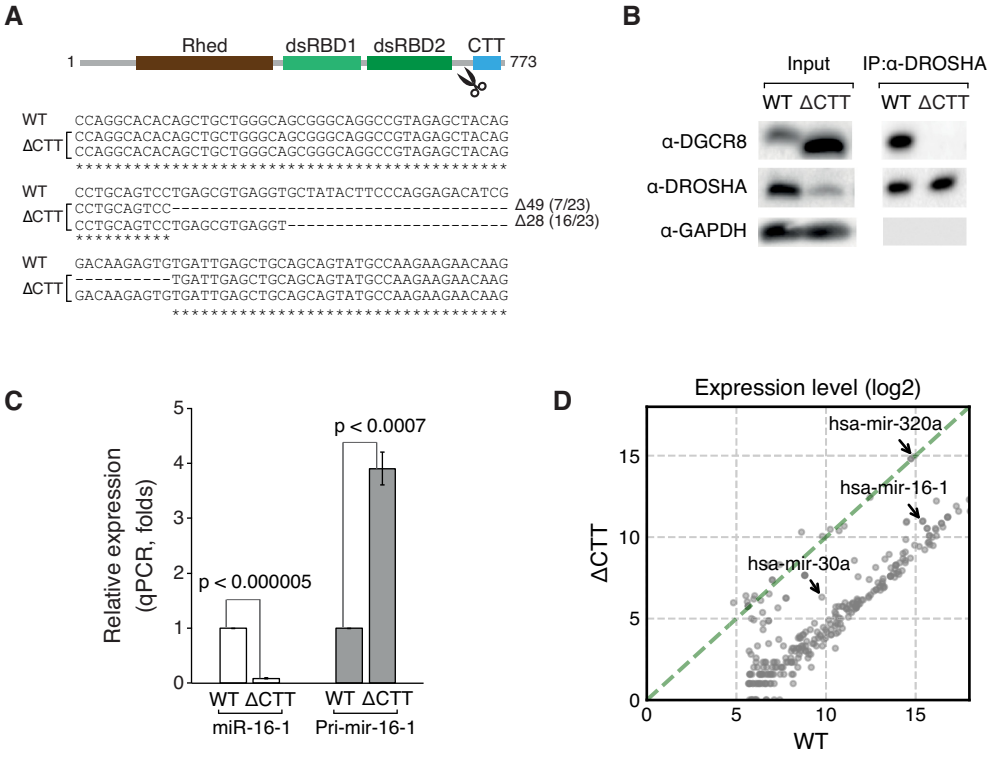

Figure 4. Generation of the DGCR8 knockout (KO) cell line. (**A**) Domain structure of DGCR8. Rhed is the RNA-binding heme domain, dsRBDs are the double-stranded RNA-binding domains, and CTT is the C-terminal tail region. The scissor indicates the genomic DNA region targeted by the nuclease. Targeted genomic sequences show the deleted region in Exon 13 of the DGCR8 gene in the DGCR8-KO (ΔCTT) cell line. The sequencing frequency of the mutated alleles in the cell clone are presented on the right. (**B**) Confirmation of the CTT deletion by Western blot and dissociation of DGCR8ΔCTT from DROSHA by co-immunoprecipitation. (**C**) The miR-16-1 and pri-mir-16-1 expression in the ΔCTT cells estimated by qPCR. The miRNA level was estimated by Taqman-based qPCR and normalized by the U6 level. The pri-mir-16-1 level was estimated by SYBR Green-based qPCR with the specific primers and normalized by the *GAPDH* mRNA level. The results were obtained from the three independent experiments. (**D**) Global analysis of miRNA expression in the ΔCTT cells. Small RNA libraries from the WT (HCT116) and ΔCTT cells were prepared as described previously (37). The abundance of miRNAs was normalized by non-canonical miRNAs: hsa-miR-320a, hsa-miR-320b-1 and hsa-miR-320c-1.

that dimeric DGCR8 enhanced processing more strongly than the monomeric DGCR8 did (15,26).

Notably, miR-16 was only modestly affected by the dimerization mutation (C352A) and not affected by the heme-binding mutation (P351A). In contrast, miR-30a was strongly dependent on DGCR8: the dimerization mutation (C352A) almost completely abrogated miR-30a processing and the heme-binding mutation (P351A) also diminished miR-30a expression (Figure 5B). This result suggests that the incorporation of hemin in DGCR8 is important for the differential expression of certain miRNAs.

To further investigate the effect of hemin, we treated the P351A-transfected cells with succinylacetone (SA), which blocks heme synthesis by inhibiting aminolevulinic acid synthase, an essential enzyme in the hemin biogenesis pathway. We found that SA treatment suppressed miR-30a expression significantly, but not miR-16a expression (Figure 5C). Moreover, the effect on miR-30a could be reversed by the addition of hemin in the culture medium (Figure 5C). We further compared pri-mir-30a with its UGU-lacking variant (pri-mir-30aΔUGU) by transfecting their expression plasmids into the ΔCTT cells together with DGCR8 expressing plasmids (Figure 5D). Wild-type pri-mir-30a processing was strongly enhanced by WT DGCR8 or P351A in hemin-supplemented cell culture (P351A-hemin). In contrast, pri-mir-30aΔUGU was only modestly enhanced by WT DGCR8 or P351A-hemin (Figure 5D). These data, together with the *in vitro* data in Figure 3, indicate the important role of hemin in differentiating the expression of UGU-containing miRNAs.

Next, we determined if hemin could induce the differential miRNA expression in a genome-wide scale. We profiled miRNA expression by small RNA sequencing in the ΔCTT cells complemented with the different DGCR8 alleles. Consistent with the miR-30a and miR-16-1 expression determined using qPCR, the WT DGCR8 strongly upregulated miRNA expression globally while the mutants had partial effects (Figure 6A and B). We next supplemented the P351A-transfected cells with 5-aminolevulinic acid (ALA), which is a heme precursor that raises the hemin concentration in cells (29). ALA increased the rescuing potency of P351A (Figure 6A and B), further supporting the conclusion that hemin is required for efficient processing of pri-miRNAs.

To examine if the mutations had a differential effect on miRNAs depending on the UGU motif, we estimated Cohen's d value between the expression levels of UGU-containing and UGU-lacking miRNAs. Cohen's d value re-

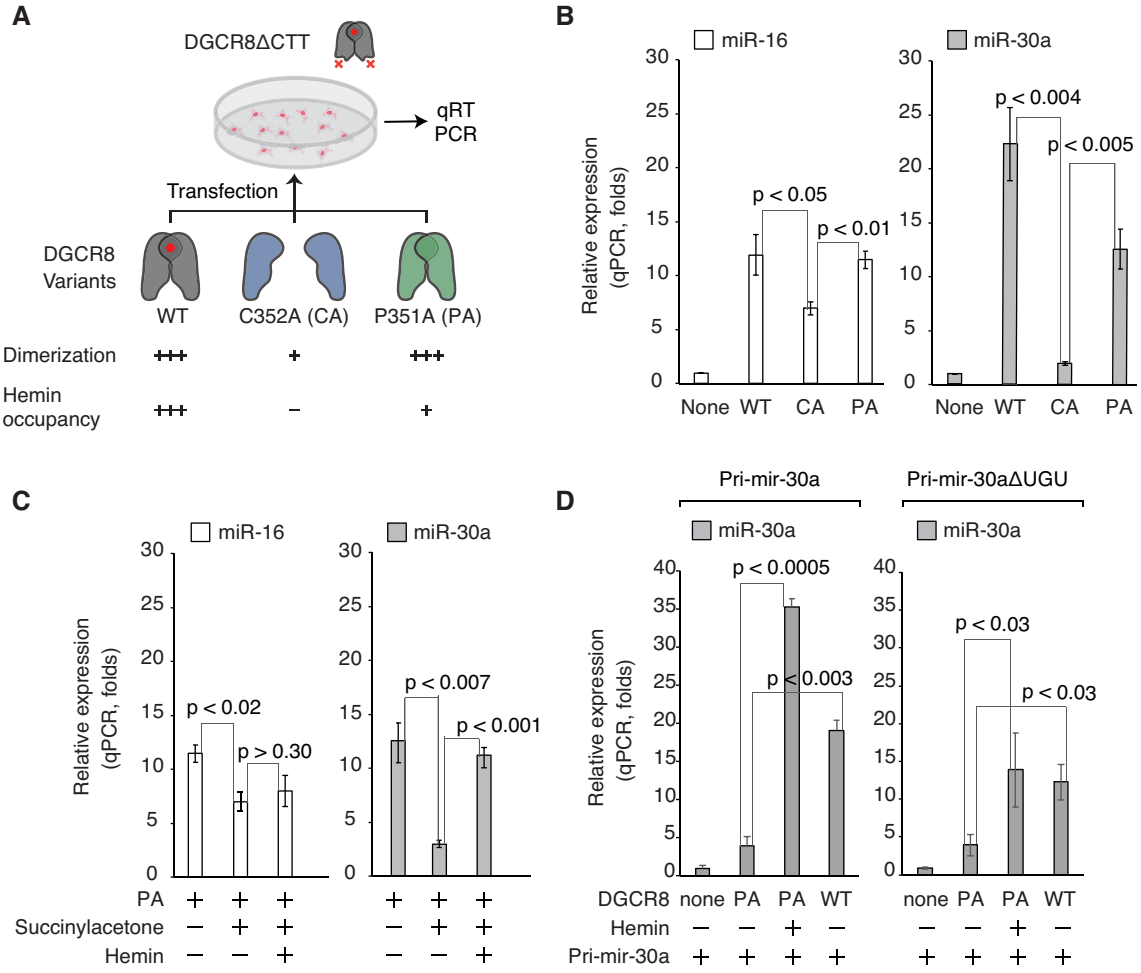

Figure 5. Hemin induces the UGU-containing miRNA expression. (**A**) The DGCR8 knockout rescue experiments. The ΔCTT cells were transfected with the pCK plasmids expressing DGCR8-WT, DGCR8-C352A, or DGCR8-P351A allele. (**B**, **C**) The miRNA expression in the rescue experiments. The miR-16-1 and miR-30a expression levels were estimated by Taqman-based qPCR and normalized by the U6 level. The results were obtained from the three independent experiments. WT: wild type DGCR8 plasmids, CA: DGCR8-C352A, PA: DGCR8-P351A. The DGCR8-P351A-transfected cells were supplemented with 0.5 mM SA 12 h post-transfection alone or were subsequently added with 2 mM hemin 24 h post-transfection. (**D**) The ΔCTT cells were transfected with the pCK plasmids expressing DGCR8-WT, or DGCR8-P351A allele along with pCDNA3 expressing pri-mir-30a or pri-mir-30aΔUGU. The DGCR8-P351A-transfected cells were either supplemented with 20 μM hemin or not. miR-30a expression levels were estimated by SYBR Green-based qPCR and normalized by the U6 level. The results were obtained from the three independent experiments. WT: wild type DGCR8 plasmids, PA: DGCR8-P351A.

flects the standardized difference between two means of two samples (41). We found that the WT significantly discriminated the UGU-containing miRNAs from the others (Figure 6C, Cohen's $d = 0.43$). In contrast, the C352A mutant failed to do so (Figure 6C, Cohen's $d = 0.06$). The P351A mutant that binds to hemin less strongly than WT was less capable of distinguishing two groups of miRNAs than WT was (Figure 6C, Cohen's $d = 0.27$). ALA treatment ameliorated this defect of the P351A mutant (Figure 6C, Cohen's $d = 0.36$). Taken together, our results indicate that the dimerization of DGCR8 is essential for recognizing the apical UGU motif of pri-miRNAs, and that hemin serves as a cofactor that reinforces the interaction between the DGCR8 dimer and the apical UGU motif.

DISCUSSION

Human Microprocessor exploits the multiple protein-RNA interactions to accurately and efficiently cleave pri-miRNAs (11,15,18). The first level involves DROSHA that recognizes and interacts with the basal ssRNA-dsRNA junction and the basal UG motif, thereby locating itself at the basal junction. However, this recognition mechanism alone is often not sufficient, and DROSHA can be misoriented at the apical junction. This leads to unproductive cleavage that does not generate any functional miRNAs. The second level of the DGCR8-RNA interaction operates to prevent DROSHA from dislocation; DGCR8 dimerizes and uses its Rhed domain to specifically interact with the apical RNA elements. This interaction allows DGCR8 to occupy the apical region of pri-miRNAs, thereby forcing DROSHA to contact the basal junction only. In this study, we introduce hemin as another level to correct the position of Micro-

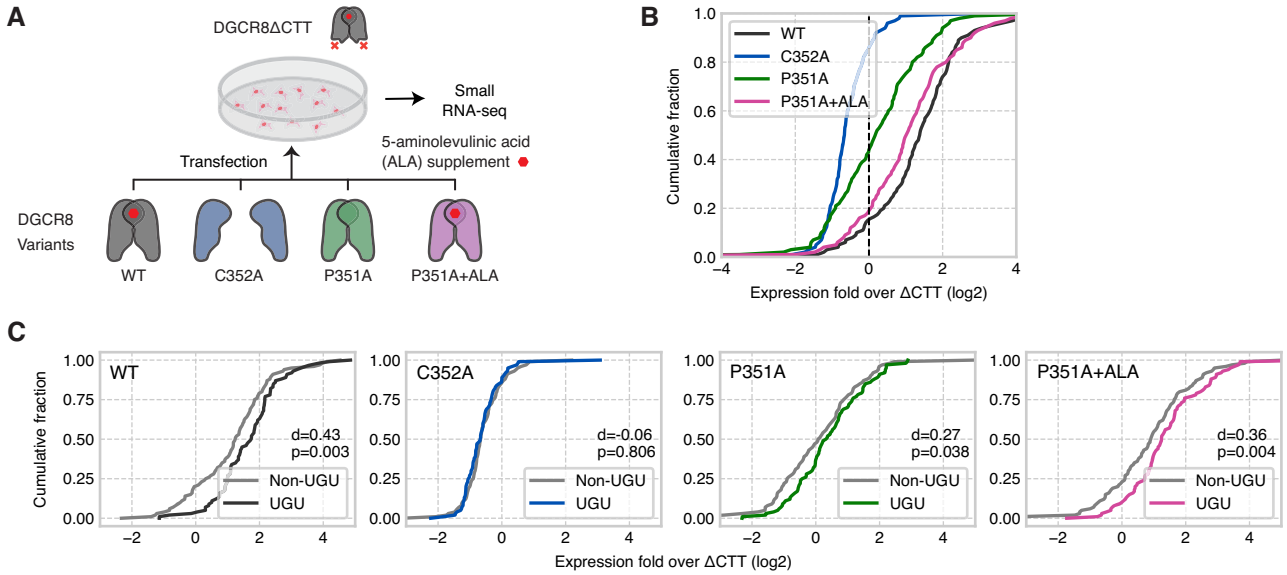

Figure 6. Hemin induces the differential miRNA expression. (**A**) The ΔCTT cells were transfected with the pCK plasmids expressing DGCR8-WT, DGCR8-C352A, or DGCR8-P351A alleles. The DGCR8-P351A-transfected cells were either supplemented with 2 mM ALA or not. (**B**) Cumulative fraction of the miRNA expression levels of the rescue ΔCTT cells. (**C**) The miRNAs were grouped by the existence of the apical UGU motif. The small RNA sequencing libraries for each transfected experiment were prepared as described previously (37), and the sequencing data analysis is described in 'Materials and Methods'.

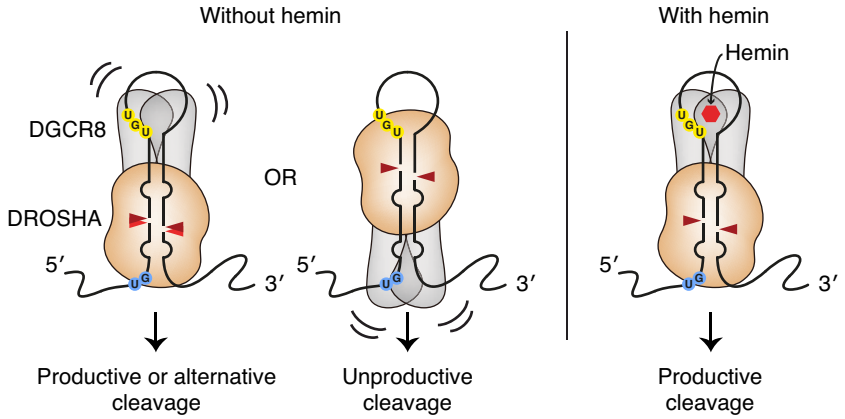

Figure 7. Molecular mechanism of hemin in pri-miRNA processing.

processor on pri-miRNAs (Figure 7 for the model). Hemin enhances the interaction between the DGCR8 dimer and UGU, thereby assisting DGCR8 in preventing DROSHA from binding at the wrong sites. Consequently, hemin increases the productive pri-miRNA processing. The action mechanism of hemin revealed in this study not only clarifies how hemin stimulates Microprocessor activity but also suggests a novel function of hemin in selectively mediating differential miRNA expression based on the UGU motif in humans. In Drosophila, the Cdk9-phosphorylated RNA polymerase II elongation complex preferentially enhances the processing of pri-miRNAs lacking the UGU motif (42). It would be interesting to study if and how RNA polymerase II-mediated miRNA regulation is connected to the hemin-dependent miRNA maturation.

Although heme and hemin are well known as major cofactors of various proteins and enzymes, the involvement of hemin in protein-RNA interaction is largely unknown. Hemin inhibits the interaction of several proteins and DNAs independently of DNA sequences (43,44). In this study, we showed that hemin stimulated sequence-specific DGCR8-RNA interaction, revealing an exciting role of hemin in the protein-RNA interaction. Structural studies will be necessary in the future to reveal the atomic details of the mechanisms underlying the hemin function in enforcing the interaction between RNA and DGCR8. It was recently reported that the conformation of DGCR8 changes upon its interaction with hemin, and that hemin helps the interaction between DGCR8 and the apical loop of pri-miRNA (36). Our current data are highly consistent with these findings, and further reveals that the UGU motif is required for the hemin-mediated stimulation of pri-miRNA processing *in vitro* and *in vivo*. The ability of hemin to differentiate cellular miRNA expression suggests a po-

tential role of hemin and the UGU motif in physiological miRNA regulation. The hemin level is controlled by multiple pathways, which can be triggered by either external or internal signals (33). It would be interesting to determine if and how UGU-containing miRNAs are regulated by the external or internal stimuli by affecting hemin levels.

SUPPLEMENTARY DATA

Supplementary Data are available at NAR Online.

ACKNOWLEDGEMENTS

We are grateful to members of our laboratories for discussion and technical assistance.

FUNDING

Institute for Basic Science from the Ministry of Science, ICT and Future Planning of Korea [IBS-R008-D1]; Hong Kong Research Grants Council [HKUST ECS26100917]. Funding for open access charge: Institute for Basic Science from the Ministry of Science, ICT and Future Planning of Korea [IBS-R008-D1].
Conflict of interest statement. None declared.

REFERENCES

1. Bartel,D.P. (2009) MicroRNAs: target recognition and regulatory functions. *Cell*, **136**, 215–233.
2. Ameres,S.L. and Zamore,P.D. (2013) Diversifying microRNA sequence and function. *Nat. Rev. Mol. Cell Biol.*, **14**, 475–488.
3. Ha,M. and Kim,V.N. (2014) Regulation of microRNA biogenesis. *Nat. Rev. Mol. Cell Biol.*, **15**, 509–524.
4. Di Leva,G., Garofalo,M. and Croce,C.M. (2014) MicroRNAs in cancer. *Annu. Rev. Pathol.*, **9**, 287–314.
5. Olson,E.N. (2014) MicroRNAs as therapeutic targets and biomarkers of cardiovascular disease. *Sci. Transl. Med.*, **6**, 239ps3.
6. Rothschild,S.I. (2014) MicroRNA therapies in cancer. *Mol. Cell Ther.*, **4**, 2–7.
7. Tutar,L., Tutar,E. and Tutar,Y. (2014) MicroRNAs and cancer; an overview. *Curr. Pharm. Biotechnol.*, **15**, 430–437.
8. Tutar,L., Tutar,E., Ozgur,A. and Tutar,Y. (2015) Therapeutic targeting of microRNAs in cancer: future perspectives. *Drug Dev. Res.*, **76**, 382–388.
9. Denli,A.M., Tops,B.B., Plasterk,R.H., Ketting,R.F. and Hannon,G.J. (2004) Processing of primary microRNAs by the microprocessor complex. *Nature*, **432**, 231–235.
10. Gregory,R.I., Yan,K.P., Amuthan,G., Chendrimada,T., Doratotaj,B., Cooch,N. and Shiekhattar,R. (2004) The microprocessor complex mediates the genesis of microRNAs. *Nature*, **432**, 235–240.
11. Han,J., Lee,Y., Yeom,K.H., Kim,Y.K., Jin,H. and Kim,V.N. (2004) The DROSHA-DGCR8 complex in primary microRNA processing. *Genes Dev.*, **18**, 3016–3027.
12. Landthaler,M., Yalcin,A. and Tuschl,T. (2004) The human DiGeorge syndrome critical region gene 8 and its D. melanogaster homolog are required for miRNA biogenesis. *Curr. Biol.*, **14**, 2162–2167.
13. Han,J., Lee,Y., Yeom,K.H., Nam,J.W., Heo,I., Rhee,J.K., Sohn,S.Y., Cho,Y., Zhang,B.T. and Kim,V.N. (2006) Molecular basis for the recognition of primary microRNAs by the DROSHA-DGCR8 complex. *Cell*, **125**, 887–901.
14. Auyeung,V.C., Ulitsky,I., McGeary,S.E. and Bartel,D.P. (2013) Beyond secondary structure: primary-sequence determinants license pri-miRNA hairpins for processing. *Cell*, **152**, 844–858.
15. Nguyen,T.A., Jo,M.H., Choi,Y.G., Park,J., Kwon,S.C., Hohng,S., Kim,V.N. and Woo,J.S. (2015) Functional anatomy of the human Microprocessor. *Cell*, **161**, 1374–1387.
16. Fareh,M., Loeff,L., Szczepaniak,M., Haagsma,A.C., Yeom,K.H. and Joo,C (2016) Single-molecule pull-down for investigating protein-nucleic acid interactions. *Methods*, **105**, 99–108.
17. Herbert,K.M., Sarkar,S.K., Mills,M., Delgado De la Herran,H.C., Neuman,K.C. and Steitz,J.A. (2016). A heterotrimer model of the complete microprocessor complex revealed by single-molecule subunit counting. *RNA*, **22**, 175–181.
18. Kwon,S.C., Nguyen,T.A., Choi,Y.G., Jo,M.H., Hohng,S., Kim,V.N. and Woo,J.S. (2016) Structure of human DROSHA. *Cell*, **164**, 81–90.
19. Ma,J.B., Ye,K. and Patel,D.J. (2004) Structural basis for overhang-specific small interfering RNA recognition by the PAZ domain. *Nature*, **429**, 318–322.
20. Macrae,I.J., Zhou,K., Li,F., Repic,A., Brooks,A.N., Cande,W.Z., Adams,P.D. and Doudna,J.A. (2006a) Structural basis for double-stranded RNA processing by Dicer. *Science*, **311**, 195–198.
21. Macrae,I.J., Li,F., Zhou,K., Cande,W.Z. and Doudna,J.A. (2006b) Structure of dicer and mechanistic implications for RNAi. *Cold Spring Harbor Symp. Quant. Biol.*, **71**, 73–80.
22. Park,J.E., Heo,I., Tian,Y., Simanshu,D.K., Chang,H., Jee,D., Patel,D.J. and Kim,V.N. (2011) DICER recognizes the 5′ end of RNA for efficient and accurate processing. *Nature*, **475**, 201–205.
23. Gu,S., Jin,L., Zhang,Y., Huang,Y., Zhang,F., Valdmanis,P.N. and Kay,M.A. (2012) The loop position of shRNAs and pre-miRNAs is critical for the accuracy of dicer processing in vivo. *Cell*, **151**, 900–911.
24. Tian,Y., Simanshu,D.K., Ma,J.B., Park,J.E., Heo,I., Kim,V.N. and Patel,D.J. (2014) A phosphate-binding pocket within the platform-PAZ-connector helix cassette of human DICER. *Mol. Cell*, **53**, 606–616.
25. Kawamata,T. and Tomari,Y. (2010) Making RISC. *Trends Biochem. Sci.*, **35**, 368–376.
26. Faller,M., Matsunaga,M., Yin,S., Loo,J.A. and Guo,F. (2007) Heme is involved in microRNA processing. *Nat. Struct. Mol. Biol.*, **14**, 23–29.
27. Barr,I., Smith,A.T., Senturia,R., Chen,Y., Scheidemantle,B.D., Burstyn,J.N. and Guo,F. (2011) DiGeorge critical region 8 (DGCR8) is a double-cysteine-ligated heme protein. *J. Biol. Chem.*, **286**, 16717–16725.
28. Barr,I., Smith,A.T., Chen,Y., Senturia,R., Burstyn,J.N. and Guo,F. (2012) Ferric, not ferrous, heme activates RNA-binding protein DGCR8 for primary microRNA processing. *Proc. Natl. Acad. Sci. U.S.A.*, **109**, 1919–1924.
29. Weitz,S.H., Gong,M., Barr,I., Weiss,S. and Guo,F. (2014) Processing of microRNA primary transcripts requires heme in mammalian cells. *Proc. Natl. Acad. Sci. U.S.A.*, **111**, 1861–1866.
30. Sassa,S. and Nagai,T. (1996) The role of heme in gene expression. *Int. J. Hematol.*, **63**, 167–178.
31. Rodgers,K.R. (1999) Heme-based sensors in biological systems. *Curr. Opin. Chem. Biol.*, **3**, 158–167.
32. Kumar,S. and Bandyopadhyay,U. (2005) Free heme toxicity and its detoxification systems in human. *Toxicol. Lett.*, **157**, 175–188.
33. Khan,A.A. and Quigley,J.G. (2011) Control of intracellular heme levels: heme transporters and heme oxygenases. *Biochim. Biophys. Acta.*, **1813**, 668–682.
34. Poulos,T.L. (2014) Heme enzyme structure and function. *Chem. Rev.*, **114**, 3919–3962.
35. Quick-Cleveland,J., Jacob,J.P., Weitz,S.H., Shoffner,G., Senturia,R. and Guo,F. (2014) The DGCR8 RNA-binding heme domain recognizes primary microRNAs by clamping the hairpin. *Cell Rep.*, **7**, 1994–2005.
36. Partin,A.C., Ngo,T.D., Herrell,E., Jeong,B.C., Hon,G. and Nam,Y. (2017) Heme enables proper positioning of Drosha and DGCR8 on primary microRNAs. *Nat. Commun.*, **8**, 1737.
37. Kim,Y.K., Kim,B.S. and Kim,V.N. (2016) Re-evaluation of the roles of DROSHA, Exportin 5, and DICER in microRNA biogenesis. *Proc. Natl. Acad. Sci. U.S.A.*, 1881–1889.
38. Marcel,M. (2011) Cutadapt removes adapter sequences from high-throughput sequencing reads. *EMBnet*, **17**, 10–12.
39. Langmead,B. and Salzberg,S.L. (2012) Fast gapped-read alignment with Bowtie 2. *Nat. Methods* **9**, 357–359.
40. Han,J., Pedersen,J.S., Kwon,S.C., Belair,C.D., Kim,Y.K., Yeom,K.H., Yang,W.Y., Haussler,D., Blelloch,R. and Kim,V.N. (2009) Posttranscriptional crossregulation between DROSHA and DGCR8. *Cell*, **136**, 75–84.

41. Jacob,C. (1988) *Statistical Power Analysis for the Behavioral Sciences*. Routledge, ISBN 1-134-74270-3.
42. Church,V.A, Pressman,S., Isaji,M., Truscott,M., Cizmecioglu,N.T., Buratowski,S., Frolov,M.V. and Carthew,R.W. (2017) Microprocessor recruitment to elongating RNA polymerase II is required for differential expression of MicroRNAs. *Cell Rep.*, **20**, 3123–3134.
43. Hernández,J.A., Peleato,M.L., Fillat,M.F. and Bes,M.T. (2004) Heme binds to and inhibits the DNA-binding activity of the global regulator FurA from Anabaena sp. PCC 7120. *FEBS Lett.*, **577**, 35–41.
44. Kaur,A.P. and Wilks,A. (2007) Heme inhibits the DNA binding properties of the cytoplasmic heme binding protein of Shigella dysenteriae (ShuS). *Biochemistry*, **46**, 2994–3000.